

Supporting information

Carbon Nano-Onion Encapsulated Cobalt Nanoparticles for Oxygen Reduction and Lithium-Ion Batteries

Ming-Jun Xiao,^a Bo Ma,^a Ze-Qi Zhang,^a Qi Xiao,^a Xiang-Yang Li,^a Zheng-Tao Zhang,^a Qiang Wang,^{*a} Yong Peng,^{*b} and Hao-Li Zhang^{*a,c}

a State Key Laboratory of Applied Organic Chemistry, Key Laboratory of Special Function Materials and Structure Design, College of Chemistry and Chemical Engineering, Lanzhou University, Lanzhou, 730000, P. R. China.

b Key Laboratory of Magnetism and Magnetic Materials of MOE, Lanzhou University, Lanzhou, 730000, P. R. China.

c Tianjin Key Laboratory of Molecular Optoelectronic Sciences, Department of Chemistry, Tianjin University, Collaborative Innovation Center of Chemical Science and Engineering (Tianjin), Tianjin 300072, P. R. China.

*Corresponding Author.

E-mail: haoli.zhang@lzu.edu.cn, qiangwang@lzu.edu.cn, pengy@lzu.edu.cn

All the density functional theory (DFT) calculations were performed by Vienna Ab-initio Simulation Package (VASP), employing the Projected Augmented Wave (PAW) method. The revised Perdew-Burke-Ernzerhof (RPBE) functional was used to describe the exchange and correlation effects. For all the geometry optimizations, cutoff energy was set to 500 eV. A $3 \times 3 \times 1$ supercell grid was used to carry out the surface calculations on the surface of carbon material. A $1 \times 1 \times 1$ supercell grid was used to carry out the surface calculations on the surface of nitrogen doped carbon material. A $3 \times 3 \times 2$ supercell grid was used to carry out the surface calculations on the surface of nitrogen doped carbon encapsulated cobalt material.

The adsorption energy E_b is defined as follows:

$$E_b = E_{\text{total}} - (E_{\text{substrate}} + E_{\text{adsorbate}}) \quad (\text{S1})$$

where E_{total} is the total energy of the adsorbate-substrate system, $E_{\text{substrate}}$ and $E_{\text{adsorbate}}$ are the energies of the (pre-adsorbed or pure) substrate, and the free adsorption, respectively, in the following adsorption.

The computational hydrogen electrode (CHE) model was used to calculate the free energy of OER, based on which the free energy of an adsorbed species is defined:

$$\Delta G_{\text{ads}} = \Delta E_{\text{ads}} + \Delta E_{\text{ZPE}} - T\Delta S_{\text{ads}} \quad (\text{S2})$$

Where ΔE_{ads} is the electronic adsorption energy, ΔE_{ZPE} is the zero point energy difference between adsorbed and gaseous species, and $T\Delta S_{\text{ads}}$ is the corresponding entropy difference between these two states.

Table S1. Charge transfer data of materials

C		C1	C2	C3	N1	Co1-2	Co2-1	Co2-2	Co3-1	Co3-2	Co4	
C	Original charge	4	4	4	0	0	0	0	0	0	0	0
	Final charge	4	4	4	0	0	0	0	0	0	0	0
	Charge transfer	0	0	0	0	0	0	0	0	0	0	0
C-N	Original charge	4	4	4	5	0	0	0	0	0	0	0
	Final charge	3.7	3.7	3.7	6.27	0	0	0	0	0	0	0
	Charge transfer	-0.3	-0.3	-0.3	1.27	0	0	0	0	0	0	0
Co-C-N	Original charge	4	4	4	5	9	9	9	9	9	9	9
	Final charge	3.75	3.68	3.75	6.14	8.9	8.9	8.9	8.9	8.9	8.92	8.9
	Charge transfer	-0.25	-0.32	-0.25	1.14	-0.1	-0.1	-0.1	-0.1	-0.1	-0.08	-0.1

C1, C2, and C3 are the three C atoms around N. Co1-1, Co1-2 are the two closest Co atoms around C1, and the other four, Co4 is the Co atom under N. Original charge is the original valence electron of ZAV in POTCAR. Final charge is the valence electron read from ACF. Charge transfer is final original, that is, valence state and gain and loss of electrons, and negative valence means loss of electrons.

Table S2. Free energy data of graphene materials.

	E(DFT)/eV	ΔG /eV	G/eV	Free-energy-eq	Free-energy/eV	U=0V	U=1.23V
ALSB	-295.2370	0.0000	-295.2370	+2H ₂ O	-323.6770	0.0000	0.0000
*OH	-303.5900	0.3430	-303.2470	+H ₂ O+1/2H ₂	-320.8670	2.8100	1.5800
*O	-298.4000	0.0425	-298.3575	+H ₂ O+H ₂	-319.3775	4.2995	1.8395
*OOH	-308.1300	0.2320	-307.8980	+3/2H ₂	-318.0980	5.5790	1.8890
SLAB	-295.2400	0.0000	-295.2400	+O ₂ +2H ₂	-318.7600	4.9170	-0.0030

Table S3. Free energy data of graphitic-NG materials.

	E(DFT)/eV	ΔG /eV	G/eV	Free-energy-eq	Free-energy/eV	U=0V	U=1.23V
ALSB	-293.2800	0.0000	-293.2800	+2H ₂ O	-321.7200	0.0000	0.0000

*OH	-303.1100	0.3373	--302.7727	+H ₂ O+1/2H ₂	-320.3927	1.3273	0.0973
*O	-298.3040	0.0523	-298.2517	+H ₂ O+H ₂	-319.2717	2.4483	-0.0117
*OOH	-307.3400	0.3853	-306.9547	+3/2H ₂	-317.1547	4.5653	0.8753
SLAB	-293.2800	0.0000	-293.2800	+O ₂ +2H ₂	-316.8000	4.9200	0.0000

Table S4. Free energy data of Co/graphitic-NG materials.

	E(DFT)/eV	ΔG/eV	G/eV	Free-energy-eq	Free-energy/eV	U=0V	U=1.23V
ALSB	-1522.4700	0.0000	-1522.4700	+2H ₂ O	-1550.9100	0.0000	0.0000
*OH	-1532.0000	0.3640	-1531.6360	+H ₂ O+1/2H ₂	-1549.2560	1.6540	0.4240
*O	-1527.8300	0.0786	-1527.7514	+H ₂ O+H ₂	-1548.7714	2.1386	-0.3214
*OOH	-1537.3100	0.5708	-1536.7392	+3/2H ₂	-1546.9392	3.9708	0.2808
SLAB	-1522.4700	0.0000	-1522.4700	+O ₂ +2H ₂	-1545.9900	4.9200	0.0000

Table S5. Adsorption energy data of graphitic-NG materials.

Adsorption energy		
*OH	*O	*OOH
-1.1327	-0.0117	-0.3547

Table S6. Adsorption energy data of grapheme materials.

Adsorption energy		
*OH	*O	*OOH
0.3500	1.8395	0.6590

Table S7. Adsorption energy data of Co/graphitic-NG materials.

Adsorption energy		
*OH	*O	*OOH
-0.8060	-0.3214	-0.9492

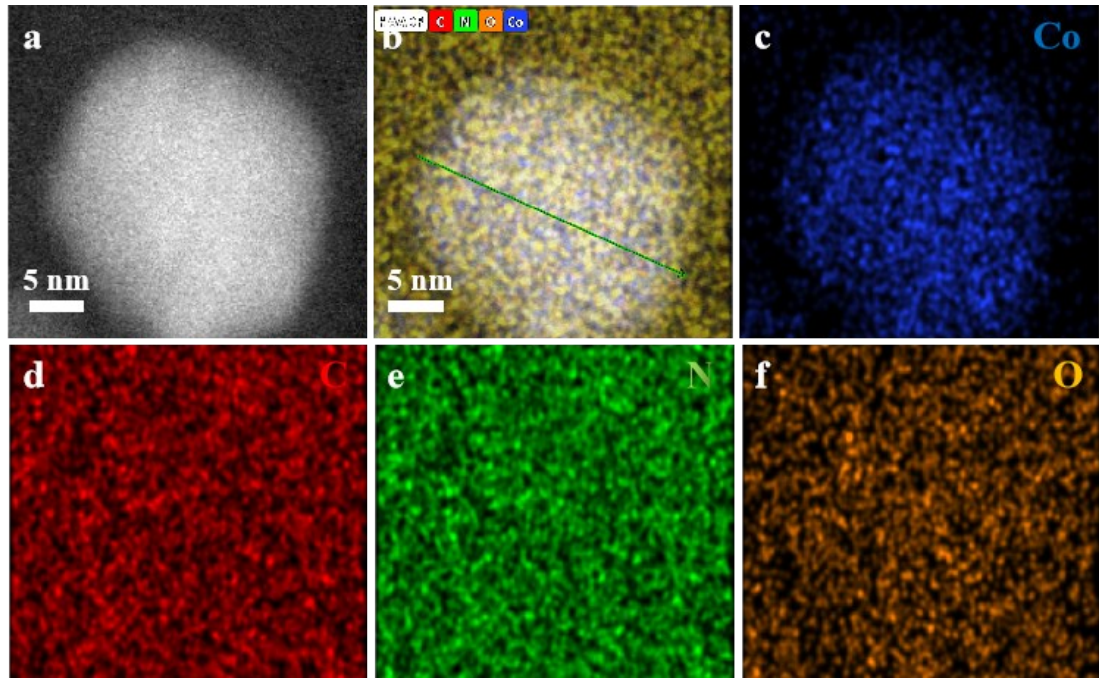


Figure S1. HADDF-STEM and EDX mapping of Co-NCNO-450 (a-f).

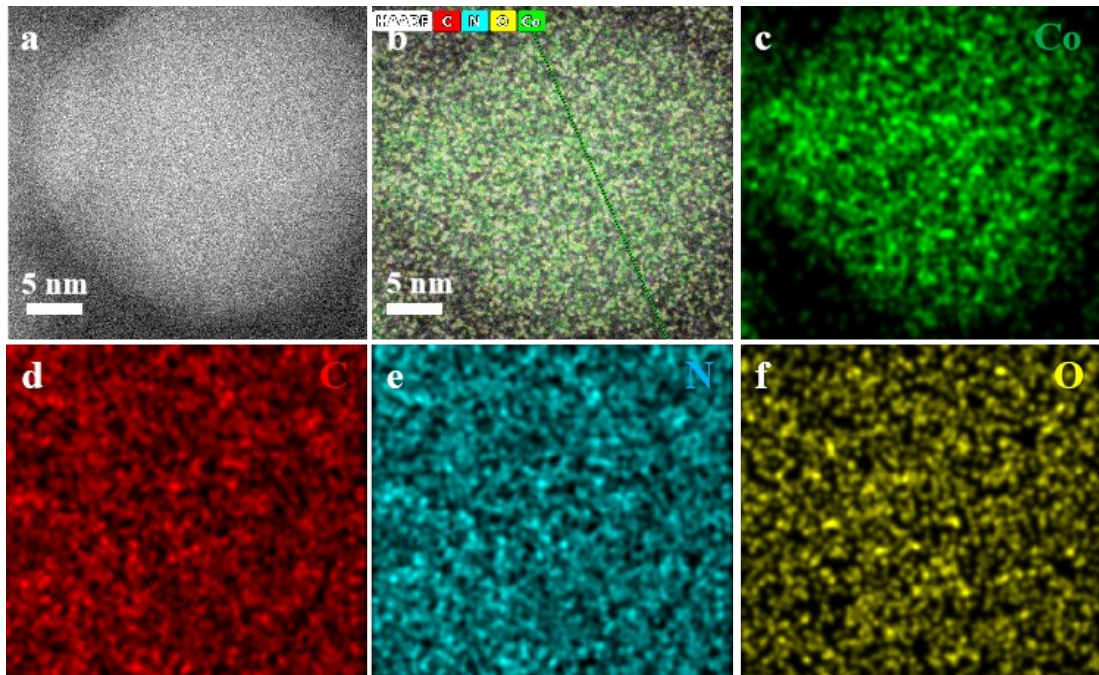


Figure S2. HADDF-STEM and EDX mapping of Co-NCNO-850 (a-f).

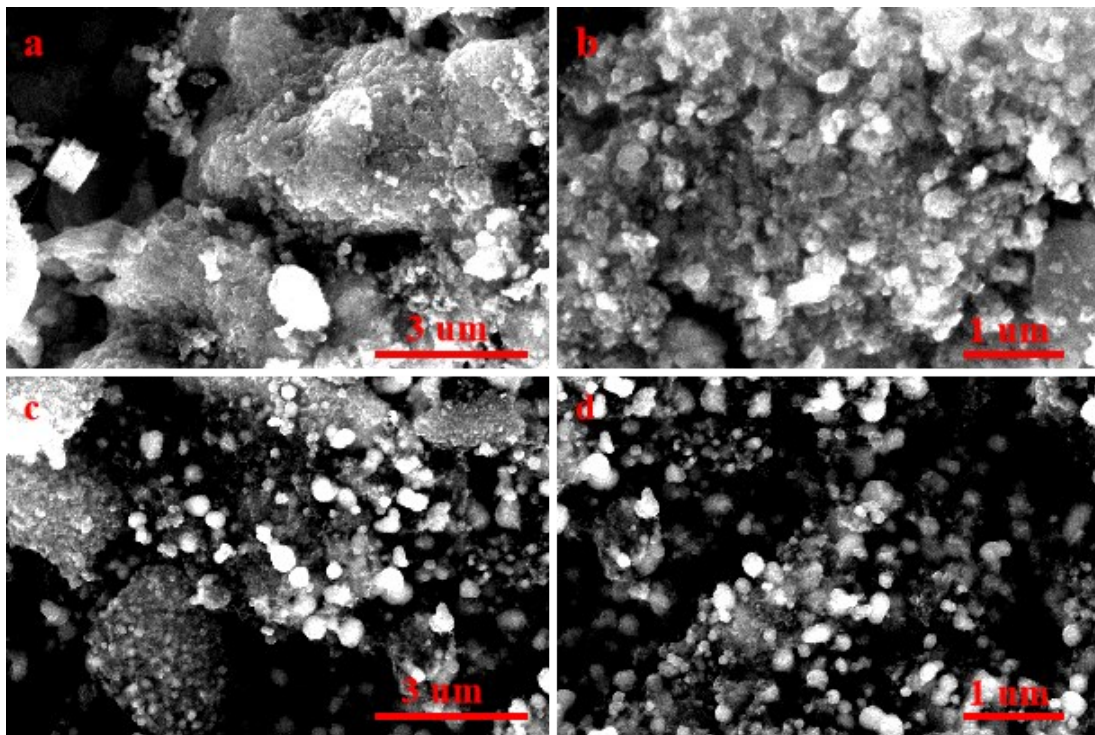


Figure S3. SEM images at different magnification of Co-NCNO-450 (a-b) and Co-NCNO-850 (c-d).

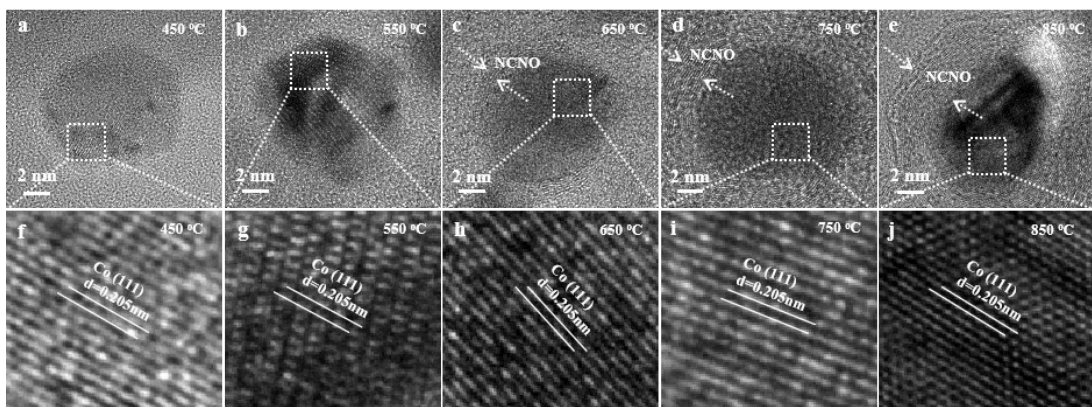


Figure S4. Ex-situ TEM (a-e) and corresponding HR-TEM (f-j) of Co-NCNO-450 from 450 °C to 850 °C.

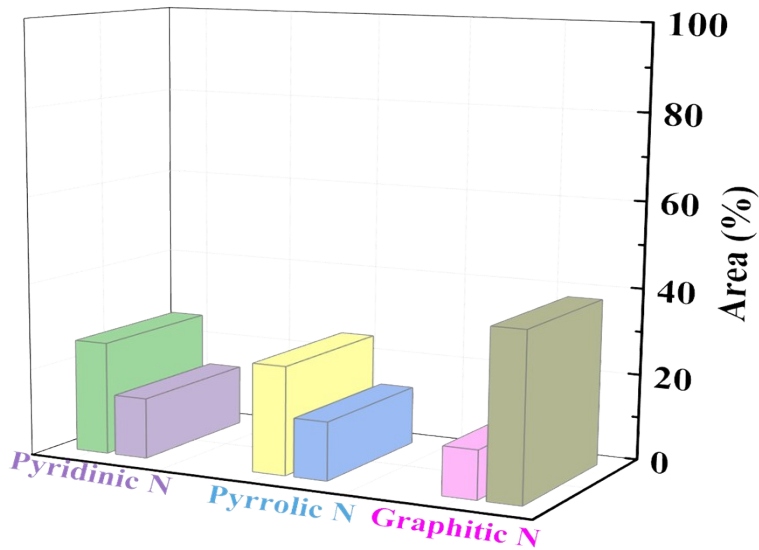


Figure S5. The content of different type nitrogen of Co-NCNO-450 and Co-NDCNO-850.

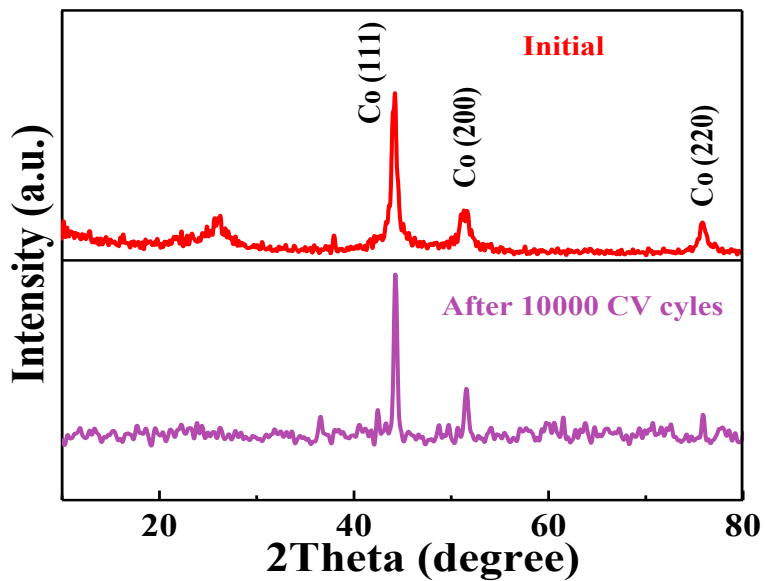


Figure S6. XRD patterns of Co-NCNO-850 before and after 10000 CV cycles.

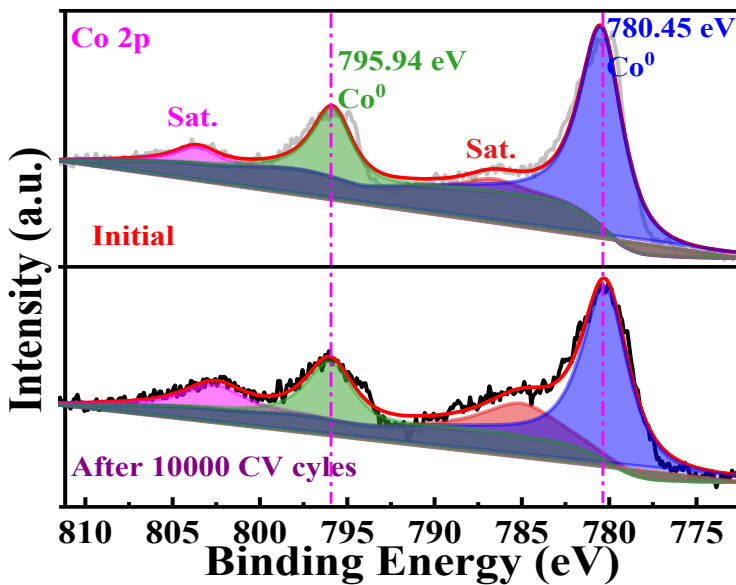


Figure S7. High-resolution XPS spectra of Co 2p of Co-NCNO-850 before and after 10000 CV cycles.

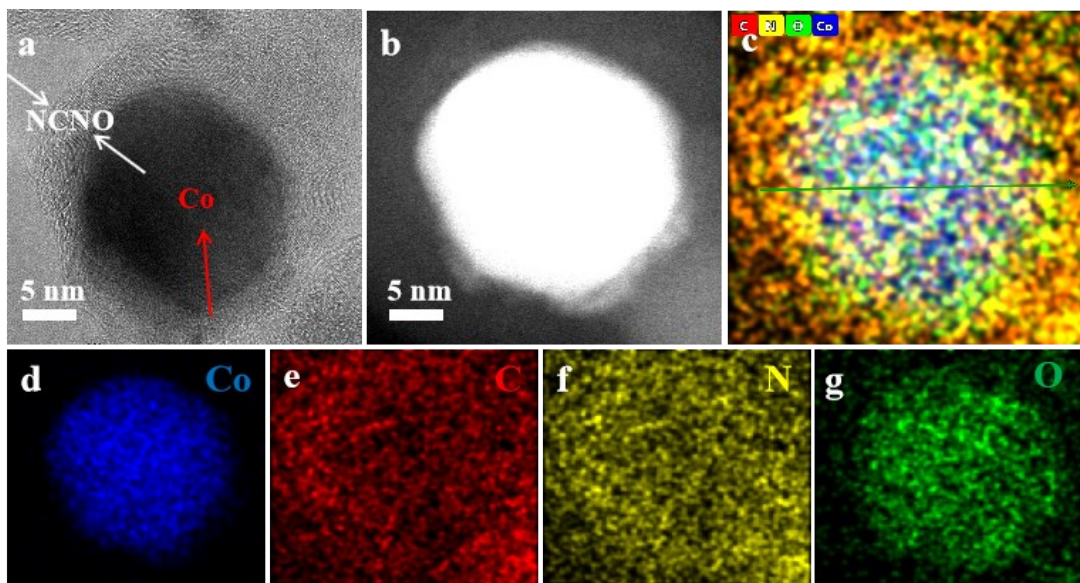


Figure S8. TEM and EDX mapping of Co-NCNO-850 (a-g) after ORR.

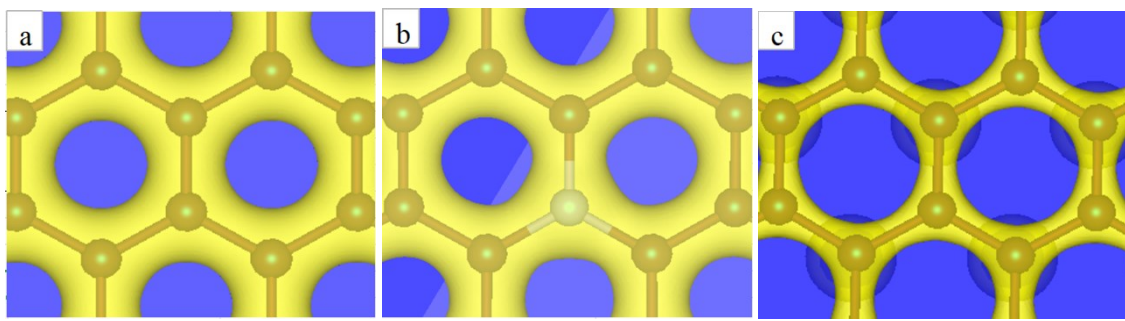


Figure S9. Charge density distribution images of graphene (a), graphitic-NG (b), Co/graphitic-NG (c).

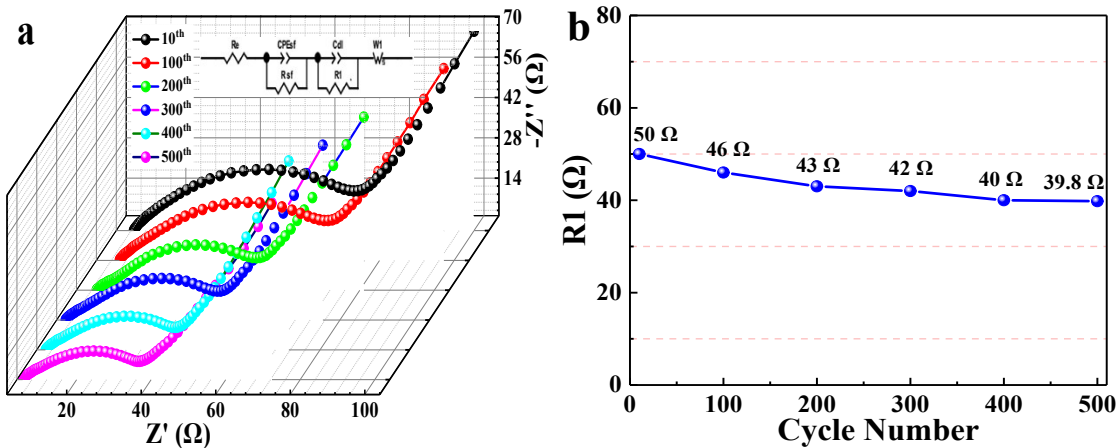


Figure S10. Nyquist plots data and fitted results (inset of the equivalent circuit) (a), charge transfer resistance of Co-NCNO-850.

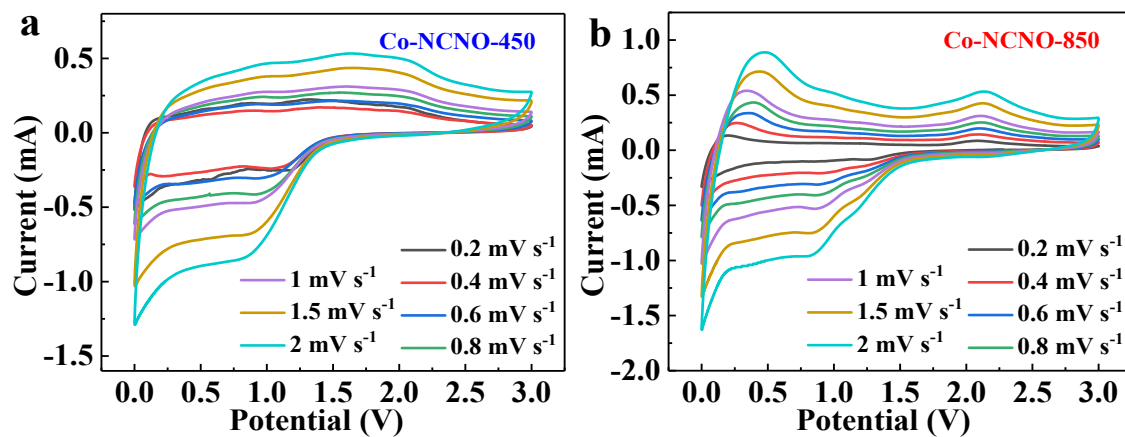


Figure S11. CV curves at different scan rates of Co-NCNO-450 (a) and Co-NCNO-850 (b).

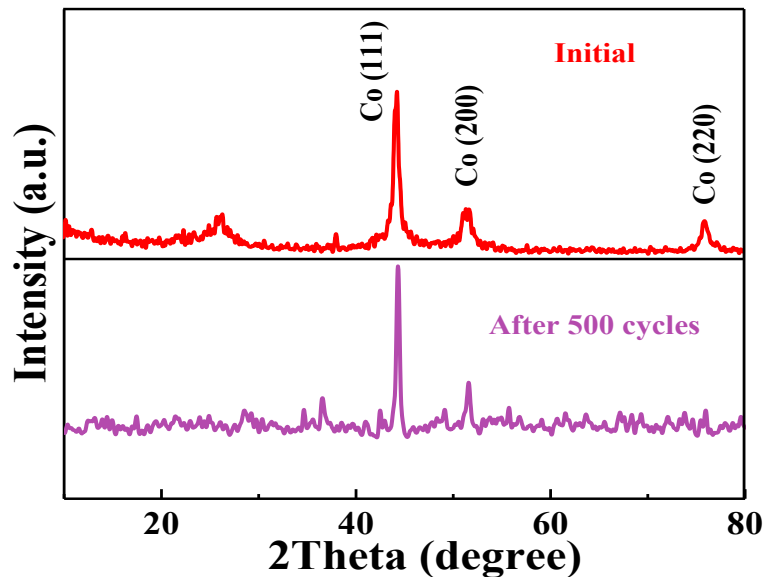


Figure S12. XRD patterns of Co-NCNO-850 initial and after 500 cycles.

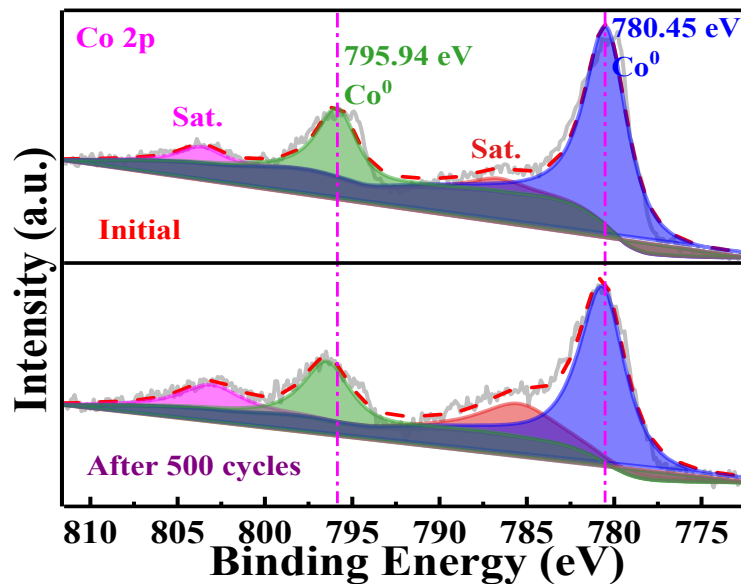


Figure S13. High-resolution Co 2p spectra of Co-NCNO-850 initial and after 500 cycles.

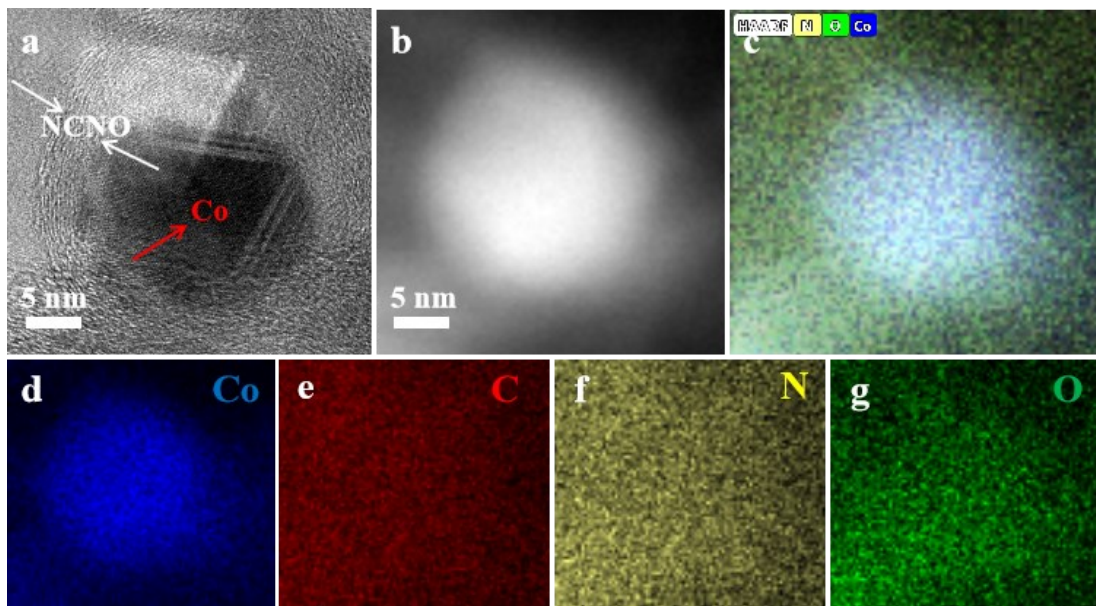


Figure S14. TEM and EDX mapping of Co-NCNO-850 (a-g) after 500 cycles at the current density of 0.5 C.

Table S8. The element content of Co-NCNO-450 and Co-NCNO-850 was obtained by XPS.

Co-NCNO-450	Element	C	Co	N
	Content	71.88 at%	8.82 at%	19.30 at%
Co-NCNO-850	Element	C	Co	N
	Content	90.13 at%	7.40 at%	2.47 at%

Table S9. The electrochemical performance comparison of the Co-NCNO with similar materials for ORR.

Materials	Method	E _{ORR} /mV (Half-wave potential)	Tafel slope/ mV/dec	References
Co@G/N-GCNs	Facile pyrolysis strategy	860	69.66	¹
Co-N-doped Carbon Nanosheets	Self-assembly strategy	930	69	²
Co@NC Core Shell Nanostructures	One-pot synthesis from Co-MOFs,	880	55	³
Co@NC-MOF	Annealing ZIF-67/PEI/GO hybrid	150	69	⁴
CS-Co/NGs	Pyrolyzing silica@CoZn imidazolate frameworks	160	86	⁵
NiN co-doped porous carbon	Treatment of g-C ₃ N ₄ incorporated ZIF-8	760		⁶

Co/N-co-doped carbon	Utilizes an octahedral Co(II) complex with 2,6-bis(benzimidazol-2-yl)pyridine (BBP)	810	7
Co-CNF	Carbonization of a newly MOFs	820	8
Co@G/C	One-step thermal treatment process	800	9
Co/N-C	Solvo-thermal carbonization strategy	61	10
Commerical Pt/C		800	
Co-NCNO-850	One-step carbonization	767	53
			Our work

Table S10. The electrochemical performance comparison of the Co-NCNO with similar materials for LIBs.

Materials	Method	Cycle number	Specific capacity (mA h g ⁻¹)	Current density (mA g ⁻¹)	References
Co/CMK-3 nanocomposites	Sonochemical method	50	720	50	11
Graphene–Ni	In-situ reduced from NiO by graphene	35	675	100	12
Co/G composites	Pyrolyzing the ZIF-67/graphene oxide composites	120	670.8	50	13
C/Co composite nano-fibers	Electrospinning and subsequent heat treatment	50	804	100	14
C/Co composite	Pyrolysis of polymeric cobalt phthalocyanine	40	600	50	15
2D Ni@PGC nanosheets		100	740	100	16
Porous graphene/Co		300	163	1000	17
Ni/C hierarchical composites	Green sol–gel route	100	635	200	18
PCC-CoO x		2000	580	1000	19
Co@PCNS	NaCl template	100	~700	500	20
Co-NCNO-850	One-step carbonization	500	774	0.5 C	Our work

References

1. H. J. Niu, L. Zhang, J. J. Feng, Q. L. Zhang and A. J. Wang, *J. Colloid Interf. Sci.*, 2019, **552**, 744-751.
2. X. Luo, X. Wei, H. Wang, Y. Wu, W. Gu and C. Zhu, *ACS Sustain. Engineering*, 2020, **8**, 9721-9730.
3. S. G. Peera, J. Balamurugan, N. H. Kim and J. H. Lee, *Small*, 2018, **14**, 1800441-1800455.

4. Q. Gao, Y. Huang, X. Han, X. Qin and M. Zhao, *Energy Technol-Ger*, 2018, **6**, 2282-2288.
5. T. Feng, H. Qin and M. Zhang, *Chemistry*, 2018, **24**, 10178-10185.
6. V. Priya K, M. Thomas, R. Illathvalappil, S. K, S. Kurungot, B. N. Nair, A. P. Mohamed, G. M. Anilkumar, T. Yamaguchi and U. S. Hareesh, *New J. Chem.*, 2020, **44**, 12343-12354.
7. S. Chao, Z. Bai, Q. Cui, H. Yan, K. Wang and L. Yang, *Carbon*, 2015, **82**, 77-86.
8. M. Kim, D.-H. Nam, H.-Y. Park, C. Kwon, K. Eom, S. Yoo, J. Jang, H.-J. Kim, E. Cho and H. Kwon, *J. Mater. Chem. A*, 2015, **3**, 14284-14290.
9. M. Sharma, J.-H. Jang, D. Y. Shin, J. A. Kwon, D.-H. Lim, D. Choi, H. Sung, J. Jang, S.-Y. Lee, K. Y. Lee, H.-Y. Park, N. Jung and S. J. Yoo, *Energy Environ. Sci.*, 2019, **12**, 2200-2211.
10. Y. Su, Y. Zhu, H. Jiang, J. Shen, X. Yang, W. Zou, J. Chen and C. Li, *Nanoscale*, 2014, **6**, 15080-15089.
11. H. Qiao, Z. Xia, Y. Liu, R. Cui, Y. Fei, Y. Cai, Q. Wei, Q. Yao and Q. Qiao, *Appl. Surf. Sci.*, 2017, **400**, 492-497.
12. Y. J. Mai, J. P. Tu, C. D. Gu and X. L. Wang, *J. Power Sources*, 2012, **209**, 1-6.
13. G.-C. Li and W. Zhao, *J. Alloys Compd.*, 2017, **716**, 156-161.
14. L. Wang, Y. Yu, P.-C. Chen and C.-H. Chen, *Scripta Mater.*, 2008, **58**, 405-408.
15. J. Yue, X. Zhao and D. Xia, *Electrochem. Commun.*, 2012, **18**, 44-47.
16. J. Zhang, H. Zhu, P. Wu, C. Ge, D. Sun, L. Xu, Y. Tang and Y. Zhou, *Nanoscale*, 2015, **7**, 18211-18217.
17. H. Cao, X. Zhou, W. Deng and Z. Liu, *J. Mater. Chem. A*, 2016, **4**, 6021-6028.
18. L. Su, Z. Zhou and P. Shen, *J. Phys. Chem. C*, 2012, **116**, 23974-23980.
19. X. Sun, G.-P. Hao, X. Lu, L. Xi, B. Liu, W. Si, C. Ma, Q. Liu, Q. Zhang, S. Kaskel and O. G. Schmidt, *J. Mater. Chem. A*, 2016, **4**, 10166-10173.
20. V. Etacheri, C. N. Hong, J. Tang and V. G. Pol, *ACS Appl. Mater. Interfaces*, 2018, **10**, 4652-4661.